Published in final edited form as:
J Neurochem. 2008 March ; 104(6): 1649–1662.

Cross-linking of sites involved with alcohol action between transmembrane segments 1 and 3 of the glycine receptor following activation

Ingrid A. Lobo[*], **R. Adron Harris**[*], and **James R. Trudell**[†]

[*] *Waggoner Center for Alcohol and Addiction Research, Section of Neurobiology and Institute for Cellular and Molecular Biology, The University of Texas at Austin, Austin, Texas, USA*

† *Department of Anesthesia, Stanford University School of Medicine, Stanford, California, USA*

Abstract

The glycine receptor is a member of the Cys-loop, ligand-gated ion channel family and is responsible for inhibition in the CNS. We examined the orientation of amino acids I229 in transmembrane 1 (TM1) and A288 in TM3, which are both critical for alcohol and volatile anesthetic action. We mutated these two amino acids to cysteines either singly or in double mutants and expressed the receptors in Xenopus laevis oocytes. We tested whether disulfide bonds could form between A288C in TM3 paired with M227C, Y228C, I229C, or S231C in TM1. Application of cross-linking (mercuric chloride) or oxidizing (iodine) agents had no significant effect on the glycine response of wild-type receptors or the single mutants. In contrast, the glycine response of the I229C/A288C double mutant was diminished after application of either mercuric chloride or iodine only in the presence of glycine, indicating that channel gating causes I229C and A288C to fluctuate to be within 6 Å apart and form a disulfide bond. Molecular modeling was used to thread the glycine receptor sequence onto a nicotinic acetylcholine receptor template, further demonstrating that I229 and A288 are near-neighbors that can cross-link and providing evidence that these residues contribute to a single binding cavity.

Keywords

alcohols; cross-linking; glycine receptor; ligand-gated ion channel; molecular modeling; transmembrane segments

The strychnine-sensitive glycine receptor (GlyR) is a member of the Cys-loop, ligand-gated ion channel family that also includes nicotinic acetylcholine receptor (nAChR), GABA type A receptor ($GABA_AR$), and 5-hydroxytryptamine type-3 ($5\text{-}HT_3R$) receptors (Ortells and Lunt 1995). GlyRs and other Cys-loop ligand-gated ion channels are composed of five subunits surrounding a central ion pore (Unwin 2005) and the transmembrane (TM) domain of each subunit is composed of four alpha helical TM segments (TM1–TM4) (Rajendra *et al.* 1997; Bertaccini and Trudell 2002; Miyazawa *et al.* 2003; Betz and Laube 2006). GlyRs are functionally diverse receptors that mediate synaptic inhibition in the CNS (Betz and Laube 2006). They are potentiated by low concentrations of alcohols and volatile anesthetics (Yamakura *et al.* 2001; Hemmings *et al.* 2005).

Address correspondence and reprint requests to R. Adron Harris, PhD, The University of Texas at Austin, Waggoner Center for Alcohol and Addiction Research, 1 University Station A4800, Austin, TX 78712-1065, USA. E-mail: harris@mail.utexas.edu.

There is a growing consensus that the overall pentameric tertiary structure shown in the cryo-electron microscopy structure of nAChR (PDB ID 2BG9) (Unwin 2005) is a suitable template for modeling most members of the Cys-loop superfamily. Recently, homology models of GlyR (Cheng *et al.* 2007a; Crawford *et al.* 2007), $GABA_AR$ (Ernst *et al.* 2005; Campagna-Slater and Weaver 2007), and a prokaryotic channel in the nAChR family (Bocquet *et al.* 2007) have been based on this template. These models trace part of their origin to the high-resolution crystal structure of an acetylcholine-binding protein (AChBP) (Brejc *et al.* 2001). The relevance of the latter structure, and a high degree of tertiary structural conservation, was recently confirmed with a high-resolution structure of the ligand-binding domain of nAChR alpha1 (Dellisanti *et al.* 2007). The present study seeks to understand conformational changes in GlyR during the transitions between the resting and the desensitized states. Of particular relevance are recent molecular dynamics (Cheng *et al.* 2007a,b) and normal mode analyses (Taly *et al.* 2005; Bertaccini *et al.* In Press) of ion channel conformational dynamics. These studies indicate the extent and direction of substantial conformational changes during the opening transition (Purohit *et al.* 2007).

Amino acids in all four GlyR TMs are hypothesized to contribute to an alcohol and volatile anesthetic drug-binding cavity, and drugs are believed to bind in the core of the alpha helical bundle (Bertaccini *et al.* 2005a; Lobo and Harris 2005). Of these amino acids, the most studied are S267 in TM2 and A288 in TM3 in the α1 subunit, which were initially identified in 1997 (Mihic *et al.* 1997). The molecular volume of the amino acids substituted for A288 were negatively correlated with volatile anesthetic action, implying that the volume of the putative drug-binding cavity is regulated by the size of the amino acid at the this position (Wick *et al.* 1998; Yamakura *et al.* 1999; Jenkins *et al.* 2001). The aligned site in the homologous $GABA_A$ receptor, A291, was shown to be surrounded by a water-filled cavity, which expanded in the presence of alcohol (Jung *et al.* 2005), and was shown to be a critical site for alcohol binding and alcohol-induced conformational changes (Jung and Harris 2006). Recent results suggest that these binding cavities are amphipathic (Bertaccini *et al.* 2007) and may extend as far as the interface with the ligand-binding domain (Mascia *et al.* 1996; Crawford *et al.* 2007).

I229 in TM1 may also be involved with volatile anesthetic action. When TM1 amino acids in the GlyR α1 subunit were converted to the corresponding anesthetic-insensitive $GA\text{-}BA_C$ ρ1 amino acids, anesthetic action was altered (Jenkins *et al.* 2001). For example, the I229F mutant was not potentiated by halothane. Mutation of the aligned site in the $GABA_A$ receptor (L232F) resulted in a receptor insensitive to halothane, but still sensitive to isoflurane. Introduction of a larger amino acid at the position (L232W) caused the receptor to be insensitive to both halothane and isoflurane (Jenkins *et al.* 2001). GlyR A288C and I229C single mutants are each able to react with thiol-specific methanethiosulfonate reagents, which function as volatile anesthetic and alcohol analogs (Lobo *et al.* 2004a). Both I229C and A288C only react in the presence of glycine, indicating that a change in receptor conformation occurs during channel gating that allows the A288C and I229C single mutants to react (Lobo *et al.* 2004a,b).

These data support the suggestion that I229 and A288 play a critical role in volatile anesthetic and alcohol action. Although both amino acids have been modeled to face one another by use of multiple bioinformatics techniques (Yamakura *et al.* 2001; Bertaccini *et al.* 2005a), the two sites have not been shown to experimentally associate in the tertiary structure of the ion channel. Previously, S267 and A288 were demonstrated to be near-neighbors because the positions can form a disulfide bond spontaneously after mutation of both amino acids to cysteines, providing evidence for a single drug-binding cavity lined by amino acids in different TMs (Lobo *et al.* 2004b).

In this study, we synthesized an I229C/A288C double mutant and tested for a direct association between I229 and A288 to assign the orientation of TM1 and TM3 using cross-linking. We used two cross-linking reagents, mercuric chloride and iodine, to examine whether cross-linking occurred between A288C in TM3 paired with a number of substituted cysteines in TM1. Mercuric chloride can cross-link vicinal pairs of cysteines to form an intermolecular mercury-linked dimer, even in TM regions with a low dielectric environment (Soskine *et al.* 2002). Iodine is an oxidizing agent, which promotes disulfide bond formation between pairs of cysteines in adjoining TM helices (Lee *et al.* 1995b; Hughson *et al.* 1997). Disulfide bonds can form between adjacent alpha helices when two cysteines are on opposing helical faces (Lee *et al.* 1995a; Soskine *et al.* 2002) and have C-alpha to C-alpha distances less than 10 Å (Yang *et al.* 1996; Winston *et al.* 2005).

The goals of the present study were: (i) to refine the orientation of residues in TM1 and TM3 with respect to the center of each subunit and (ii) to decide how to align residues in TM3 of the GlyR with the corresponding residues in the nAChR. Although the structure of the *Torpedo* nAChR at 4 Å resolution was a major advance in understanding the tertiary structure of all Cys-loop ligand gated ion channels (Miyazawa *et al.* 2003; Unwin 2005), there are significant questions about the orientation (Campagna-Slater and Weaver 2007) and dynamics of the TM segments (Paas *et al.* 2005; Bertaccini *et al.* In Press). For example, it has been proposed that the highly conserved proline near the center of TM1 in the homologous $5HT_{3A}$ receptor could undergo a *cis-trans* isomerization, thereby changing the orientation of the extracellular half of TM1 (Dang *et al.* 2000; Lester *et al.* 2004). This 'kinking' would be consistent with previous photolabeling (Blanton and Cohen 1994) and cysteine mutagenesis (Akabas and Karlin 1995) studies that interpreted TM1 as having an irregular, non-helical structure (Leite *et al.* 2000).

In regard to the second goal, Bertaccini and Trudell (2002) suggested a single gap after GlyR K281 in the alignment of residues between the extracellular end of TM2 and the intracellular end of TM3 in the nAChR. Recently, Sieghart and coworkers proposed that $GABA_A$Rs (and presumably also GlyRs) should have two gaps inserted before TM3 in the alignment with the nAChR (Ernst *et al.* 2005; Sarto-Jackson *et al.* 2007). The additional gap would have the effect of moving GlyR A288 100 degrees clockwise (and intracellular) toward the center of the subunit. Using a completely different approach based on hydrophobicity of the TM domain alpha helices, Campagna-Slater and Weaver (2007) suggested a similar alignment of the $GABA_A$R with the nAChR. The results of cross-linking between TM1 and TM3 described in this study will help resolve these issues.

Materials and methods

Mutagenesis and expression of human GlyR α1 subunit cDNA

Missense mutations were introduced in the human GlyR α1 subunit (subcloned in the pBKCMV N/B-200 vector) using the Quik-Change site-directed mutagenesis kit (Stratagene, La Jolla, CA, USA). Point mutations were verified by partial sequencing of the sense and antisense strands. *Xenopus laevis* oocytes were isolated and injected (1 ng per 30 nL) with either human GlyR α1wild-type (WT), α1 mutant M227C, I229C, S231C, A288C, C290S, M227C/A288C, Y228C/A288C, I229C/A288C, P230C/A288C, S231C/A288C, M227C/C290S, S231C/C290S, I229C/A288C/C290S cDNAs or I229C + A288C cDNAs in a 1:1 ratio. GlyR α1 subunits assemble homomerically when expressed in a heterologous system, such as *Xenopus laevis* oocytes, to form functioning receptors with properties like those of native receptors (Taleb and Betz 1994).

The use of *Xenopus laevis* frogs was in accordance with the National Institutes of Health guide for the care and use of laboratory animals. Ovarian tissue was placed in modified Barth's

solution (MBS) containing 88 mmol/L NaCl, 1 mmol/L KCl, 10 mmol/L HEPES, 0.82 mmol/L $MgSO_4$, 2.4 mmol/L $NaHCO_3$, 0.91 mmol/L $CaCl_2$, and 0.33 mmol/L $Ca(NO_3)_2$, and adjusted to pH 7.5. Following manual isolation of *Xenopus laevis* oocytes with forceps, oocytes were treated for 10 min with collagenase type 1A solution, containing 0.5 mg/mL collagenase, 83 mmol/L NaCl, 2 mmol/L KCl, 1 mmol/L $MgCl_2$, and 5 mmol/L HEPES, adjusted to pH 7.5. Nuclear injection of cDNA was performed using a microdispenser (Drummond Scientific, Broomwall, PA, USA). Injected oocytes were singly stored in incubation media, composed of MBS supplemented with 10 mg/L streptomycin, 10 000 U/L penicillin, 50 mg/L gentamicin, 90 mg/L theophylline, and 220 mg/L sodium pyruvate (Sigma Chemical Co., St Louis, MO, USA) at 13°C.

Electrophysiology

Electrophysiological measurements were made at room temperature (23°C) in oocytes 1–10 days following injection. Oocytes were placed in a rectangular chamber, with a volume of approximately 100 μL, and perfused with MBS at a rate of 2.0 mL/min with a peristaltic pump (Cole-Parmer Instruments Co., Chicago, IL, USA) through 18-gauge polyethylene tubing (Becton Dickinson, Sparks, MD, USA). Oocytes were impaled in the animal pole with two glass electrodes filled with 3 mol/L KCl and clamped at −70 mV using a Warner Instruments OC725C (Hamden, CT, USA) oocyte clamp. Currents were continuously plotted using a chart recorder (Cole-Parmer Instrument Co.). For each experiment, recordings used oocytes from at least two different frogs.

The responses of WT and mutant GlyRs to glycine (Biorad, Hercules, CA, USA), ranging in concentration from 10 μmol/L to 10 mmol/L, were tested to generate glycine concentration–response curves. Glycine was dissolved in MBS and applied for 20 s (30 s for lower concentrations). Washout times were 10 min when glycine gave no response or a small response and were 15–20 min long after applying glycine solutions of the EC_{50} or greater. Concentration–response curves were individually fitted for each cell with non-linear curve regression for sigmoidal dose–response curves with a variable slope. The individual EC_{50} and Hill coefficient values were then averaged for each receptor. Maximal glycine responses were determined from the concentration–response curves, and these concentrations were used in the cross-linking experiments.

Dithiothreitol (DTT; Sigma-Aldrich Co., St. Louis, MO, USA) was freshly prepared at a concentration of 10 mmol/L prior to each 3 min application. Mercuric chloride ($HgCl_2$; 10 μmol/L; Sigma-Aldrich Co.) was prepared from a 1 mmol/L stock in MBS and applied to cross-link (Soskine *et al.* 2002) for 1 min. Iodine (I_2; 0.5 mmol/L) was prepared from a 1 mmol/L stock in dimethyl sulfoxide and applied for 1 min. Solutions containing DTT, $HgCl_2$, and I_2 were prepared in either MBS or glycine solutions. Cross-linking experiments were performed as follows: maximal glycine was applied twice, followed by application of iodine (0.5 mmol/L, 1 min), a maximal glycine application, reduction with DTT (10 mmol/L, 3 min), and a final maximal glycine application. There were 15 min of washout in MBS between each application. The oocyte was unclamped to preserve its health during application of oxidizing/cross-linking and reducing compounds. Oocytes were re-clamped 5 min after cross-linking or reduction applications, washed in MBS for 10 min, and maximal glycine responses were then tested. For each mutant, the effect of cross-linking and reducing agents were tested on the maximal glycine response, determined from concentration–response curves. Strychnine (10 μmol/L; Sigma-Aldrich Co.) was prepared from a 1 mmol/L stock in MBS and applied for 40 s.

Data analysis

Data analysis was performed using GraphPad Prism, Version 4.03 (GraphPad Software Inc., San Diego, CA, USA). The Student's *t*-test and one-way ANOVA were used to define statistical significance.

Molecular modeling

The 4 Å resolution cryo-electron microscopy structure of the *Torpedo* nAChR alpha subunit (PDB ID 2BG9) (Unwin 2005) was used as a template for preparation of models of a GlyR alpha subunit. The PDB file for the 4 Å structure of 2BG9 (Unwin 2005) was edited to provide a single nAChR alpha subunit as a template for the GlyR TM domain. The primary sequence of GlyR alpha 1 was threaded onto the backbone atoms of the nAChR template (PDB ID 2BG9) and the positions of the side chains were optimized while the backbone atoms were tethered (Crawford *et al.* 2007). Initially, a GlyR subunit was built with our previously suggested one-gap alignment between the GlyR and the nAChR using Discovery Studio 1.7 (Accelrys, San Diego, CA, USA). The distances between the C-alpha to C-alpha carbons of A288 in TM3 and residues in TM1 were measured. Then models corresponding to the two-gap insertion in the alignment of TM3 between the $GABA_AR$ (and presumably GlyR) with nAChR suggested by Seighart and coworkers (Ernst *et al.* 2005; Sarto-Jackson *et al.* 2007) were built. The models were examined visually and the inter-residue distances were measured. The additional gap after GlyR K281 had the effect of rotating A288C 100 degrees clockwise with respect to the long axis of the TM3 alpha helix, as viewed from the extracellular end. This position is consistent with the hydrophobicity profile suggested recently (Campagna-Slater and Weaver 2007). We found that the two-gap TM3 model had the closest inter-residue distance between I229C and A288C. We then built a series of models in which gaps were inserted in TM1 after GlyR G221. Each additional gap had the effect of rotating the residues by 100 degrees clockwise with respect to the long axis of the TM1 alpha helix, as viewed from the extracellular end. We selected the best model based on the distance between the C-alpha to C-alpha carbons of A288C in TM3 and I229C in TM1.

Helical wheel diagram of GlyR

A helical wheel of a four-helical bundle was prepared and then duplicate images were added with a 72 degree rotation about the ion pore axis to form a homopentamer. Heptads of one four-helical GlyR subunit were retained as well as the two counterclockwise heptads (TM1a and TM2a) and two clockwise heptads (TM2b and TM3b). The position of each residue in the eight heptads was linked to an Excel spreadsheet. This arrangement allowed 'what if' experiments by cutting and pasting residues in the spreadsheet and then updating the links.

Results

Concentration–response data

The homomeric WT and mutant α1GlyRs were tested for their responses to glycine in concentration–response curves. The glycine EC_{50} values, the Hill coefficients, and maximal currents for the mutants were compared with the WT receptor (Table 1). Receptors containing the A288C mutation were all less sensitive to glycine, except for the I229C/A288C double mutation, which was similar in sensitivity to the WT receptor. Mutations containing the S231C mutation were also significantly less sensitive to glycine. Coupling A288C and S231C resulted in the least sensitive receptor tested. There were no significant differences in the Hill coefficients and maximal glycine responses because of the introduced cysteines.

The glycine concentration–response curves were used to determine the maximal glycine responses for each receptor. For the WT, I229C, M227C, C290S, M227C/A288C, M227C/

C290S, I229C/A288C, I229C/A288C/C290S receptors, the maximal glycine responses was elicited with 1 mmol/L glycine. For A288C, S231C, Y228C/A288C, S231C/A288C, S231C/C290S receptors, 10 mmol/L glycine was required to elicit a maximal response. These maximal concentrations of glycine were used in the following cross-linking experiments.

Intrasubunit cross-linking of I229C with A288C

We tested for cross-linking using iodine (0.5 mmol/L) applied either in MBS or in maximal glycine (as above). WT receptor glycine responses were unchanged by application of I_2 and DTT in either the absence or presence of glycine. A tracing of the WT responses in an experiment where I_2 and DTT were applied in the presence of glycine is shown in Fig. 1a. I229C/A288C receptors reacted with iodine only in the presence of glycine, resulting in a decreased glycine response (Fig. 1b). Following reduction with DTT in glycine, the I229C/A288C receptor response was significantly larger than in cross-linked receptors ($p = 0.036$), but did not completely recover to the initial glycine response. In contrast, there was no evidence that disulfide bonds formed when iodine was applied in the absence of glycine (Fig. 1c). The I229C and A288C single mutants did not react with either iodine alone, or with iodine in the presence of glycine. Summarized data for the WT, single mutants and the I229C/A288C double mutant are shown in Table 2. Glycine responses of each oocyte were normalized to the initial glycine response, where the initial response was set to equal 1.00. The responses of all oocytes in an experiment were averaged. Subsequent glycine responses were compared with the respective initial glycine response, which is not shown in Table 2.

A second set of experiments used the cross-linking reagent $HgCl_2$. Here, cross-linking and reduction experiments were carried out in the presence of glycine. As with I_2, the WT, I229C, and A288C receptors showed no response to application of $HgCl_2$ or DTT. However, the I229C/A288C double mutant was cross-linked by $HgCl_2$, resulting in a decreased glycine response. The I229C/A288C glycine response was restored to initial values following reduction with DTT, applied in the presence of glycine. The normalized glycine responses for these experiments are summarized in Table 3.

Effect of cross-linking on GlyR I229C/A288C leak current, tonic activity, and baseline current

The I229C/A288C mutant did not show any indication of tonic activity before cross-linking. Upon re-clamping oocytes expressing I229C/A288C receptors after oxidation in the presence of glycine, a large, inward leak current was present. The current declined to a stable baseline within 10–15 min. The latter baseline was shifted from the initial pre-cross-linking initial baseline, suggesting that, in the absence of glycine, I229C/A288C receptors were tonically open following cross-linking. The WT receptor did not show a leak current or large baseline shift following oxidation. In order to examine the tonic activity, we applied the channel antagonist strychnine (10 μmol/L, 40 s) to I229C/A288C or WT receptors both before and after oxidation. WT GlyRs did not respond to strychnine in the absence of glycine. Following cross-linking, strychnine application resulted in a decrease of the I229C/A288C tonic inward current, indicating that channels were open in the absence of glycine (Fig. 2a and b). The baseline shift following cross-linking corresponded to tonic activity in the I229C/A288C receptors, confirming that a spontaneous inward leakage current was present. This mean shift in baseline was significantly different from the WT receptors (Fig. 2c).

Auto-oxidation and intersubunit cross-linking do not occur between I229C and A288C

We tested whether auto-oxidation occurred in the I229C/A288C double mutant upon repeated applications of maximal glycine. There was no decrease in current upon repeated glycine exposures, indicating that disulfide bonds could not form during channel gating without the presence of cross-linking or oxidizing agents. Additionally, exposure to DTT (10 mmol/L) in 1 mmol/L glycine did not increase the current of a subsequent glycine application (Fig. 3a).

We tested for the possibility of intersubunit cross-linking between co-injected single mutant I229C and A288C receptors. There was no observed change in current following application of iodine and glycine in cells co-injected with a 1:1 ratio of I229C and A288C single mutants, indicating that intersubunit cross-linking does not occur (Fig. 3b). Additionally, we tested a final control to see whether removal of the one native cysteine in the TM domain, C290, altered disulfide bond formation. The I229C/A288C/C290S triple mutant responded to iodine oxidation in the same manner as I229C/A288C receptors, indicating that C290 played no role in cross-linking either I229C or A288C (Fig. 3c).

Reaction of pairs of cysteines in TM1 and TM3 and single mutants

After establishing that disulfide bond formation occurred between I229C and A288C, we tested a series of double mutants that paired A288C with introduced cysteines at sites that neighbored I229 in TM1. These mutants included M227C/A288C, Y228C/A288C, P230C/A288C and S231C/A288C.

P230C/A288C receptors expressed poorly, and we were unable to obtain a glycine concentration–response curve. For the few oocytes that responded to glycine, the currents were very small and showed rapid desensitization. These currents were unaffected by DTT (10 mmol/L, 3 min) treatment (data not shown). The Y228C/A288C mutant did not show any change in glycine response following application of iodine in the presence or absence of glycine (Fig. 4a). Lastly, the M227C/A288C and S231C/A288C mutants both showed a diminished glycine-induced currents following application of iodine (Table 4). As noted below, the C-alpha to C-alpha distances of M227C/A288C and S231C/A288C are 15.0 and 17.2 Å. These C-alpha to C-alpha distances are considerably greater that the 12.4 Å distance of I229C/A288C. However, it should be noted that, in a much less conformationally constrained four-helical bundle, formation of di-cysteine cross-links over distances of 20 Å were possible (Winston *et al.* 2005). As we did not expect these two pairings to form disulfide bonds, we examined the single mutants. Both the M227C and S231C single mutants also showed decreased glycine-induced responses after application of iodine in either the presence or absence of glycine, indicating that these introduced cysteines did not react with A288C (Table 4).

M227C and S231C single mutants do not form disulfide bonds with the native cysteine in the TM domain

There is one native cysteine, C290, in the TM domain. As this position was non-reactive with methanethiosulfonate reagents (Mascia *et al.* 2000) and did not show evidence of cross-linking with the I229C and A288C single mutant controls, we believed this position was in a lipid-facing or non-reactive position, facing away from the drug-binding cavity. As both the M227C and S231C single mutants showed altered glycine responses after application of iodine, we removed the native cysteine to test whether cross-linking was occurring between either the M227C or the S231C single mutant and C290 in an adjacent α1 subunit. We found that the M227C/C290S and S231C/C290S mutants both showed cross-linking in the same manner as their respective TM1 single mutants, indicating that the TM1 cysteines were not forming disulfide bonds with C290 (Fig. 4b and c). We could not identify the reason for reaction of the M227C and S231C single mutants with iodine. Removal of the native cysteine alone (C290S) resulted in a channel with glycine responses indistinguishable from the WT receptor (Table 1). Additionally, like the WT, glycine responses were unchanged in the C290S mutant after application of either iodine or DTT (Table 4).

Results of molecular modeling

The ability to cross-link I229C/A288C provided new information about the likely orientation of these two residues in GlyR. Our previous alignment of GlyR with nAChR required gaps to be placed in each primary sequence in order to optimize the overall alignment scores and reach

a consensus among different algorithms for predicting TM alpha helices (Bertaccini and Trudell 2002). Figure 5 shows a new alignment that is most consistent with experimental data. Our initial alignment of the TM1 segments placed two gaps in GlyR TM1 corresponding to nAChR P211 and L212. However, in order to have the side chain of GlyR L229 face into the interior of the four-helical bundle using the Unwin structure (PDB ID 2bg9) as a template, we added 2 extra gaps to that space, aligning GlyR I229 with nAChR C222. We aligned TM2 starting at nAChR E241 (GlyR A251), as we described previously (Bertaccini and Trudell 2002) and as is generally accepted (Ernst *et al.* 2005). We inserted two gaps before TM3, corresponding to nAChR P272 and L273 (Fig. 5). This is the alignment preferred by Ernst *et al.* We omitted the TM3–TM4 cytoplasmic loop, as little is known about its structure (Ernst *et al.* 2005; Campagna-Slater and Weaver 2007). In Fig. 5, we show an alignment of TM4 starting at nAChR K400, although we predicted that it would start at nAChR H408 (Bertaccini and Trudell 2002). As recently reviewed (Ernst *et al.* 2005; Campagna-Slater and Weaver 2007), homology is low in TM4s over the whole Cys-loop superfamily. Even using a consensus of 10 algorithms specifically designed to find TM alpha helices, we found wide variation in the predicted TM4 segments (Bertaccini and Trudell 2002). We considered three alignments: First, we previously used the set of conserved positive residues at the beginning of TM4 as an alignment point [acetylcholine receptor (AChR) H408 with GlyR R392] (Bertaccini and Trudell 2002). Second, Ernst *et al.* (2005) used the conserved negative residues at the beginning of TM4 as an alignment point (AChR D407 with GlyR D388). Third, we based an alignment on the experimental data that GlyR W407 and Y410 faced into a water-filled inter-helical cavity (Lobo *et al.* 2006) and were especially sensitive to mutations (Jenkins *et al.* 2001). This result, shown in Fig. 5, aligns AChR G421 and S424 with GlyR W407 and Y410. Three dashes were inserted at the predicted extracellular end of TM4 to indicate the beginning of a short C-terminus.

Shown in Fig. 6a is a model of a GlyR subunit built by direct substitution of GlyR residues onto the corresponding residues in the nAChR 2BG9 structure using our previous alignment between GlyR and nAChR (Bertaccini and Trudell 2002). Visual inspection of the C-alpha to C-alpha dimensions showed they were much greater (18.3 Å) than those that would provide an ideal unstrained di-cysteine cross-link. In Fig. 6a, the side chain of A288C faces away from the subunit center and into the surrounding lipid membrane. This orientation is contrary to our ability to cross-link GlyR A288 with S267, a residue known to face the interior of the GlyR subunit (Lobo *et al.* 2004b). As a result, we accepted the two-gap alignment of TM3 in all subsequent models that examined the structure of TM1. Based on the present experimental results of TM1 mutations in oocytes (Tables 1–3) and previous demonstrations of the effects of mutations at the I229 position on anesthetic sensitivity (Jenkins *et al.* 2001), we focused on the C-alpha to C-alpha distance between GlyR A288C and I229C. We found that the combination of a model with two gaps after GlyR G221 and two gaps after K281 (Fig. 5) produced the shortest C-alpha to C-alpha distance between A288 and sites in TM1 (12.4 Å, Fig. 6b). In that M227C and S231C were also of interest, we measured the corresponding C-alpha to C-alpha distances to A288 (15.0 and 17.2 Å).

The helical wheel diagram shown in Fig. 7 shows the likely spatial relationships of the amino acid residues in one four-helical bundle and the nearest neighbors on each side. The present arrangement reflects the alignment in Fig. 5 and the two-gap model shown in Fig. 6. The residues most important for effects of alcohols and anesthetics were assigned a ‘D’ position in each heptad (I229, S267, A288, and W407). Because the position of each residue in the eight heptads was linked to an Excel spreadsheet, the arrangement allowed ‘what if’ experiments by cutting and pasting residues in the spreadsheet and then updating the links. This arrangement helps explain the ability of I229C/A288C to cross-link, but suggests that intersubunit cross-linking of M227C/A288C or S231C/A288C would require substantial movements or re-arrangements of the helical segments.

Discussion

In the present study, we used di-cysteine cross-linking to address two points of controversy about the structure of GlyRs: What is the correct orientation of GlyR I229 (and therefore P230) in TM1 and A288 in TM3 with respect to the putative anesthetic/alcohol-binding site in the center of the subunit and the lumen of the ion channel? What is the correct alignment of the GlyR sequence with nAChR?

These results indicate that intrasubunit cross-links form between I229C and A288C only in the presence of glycine with an oxidizing or cross-linking reagent. This ability to cross-link means that the alpha carbons of I229 and A288 fluctuate to be approximately 6 Å apart during the transitions between the resting and desensitized states of the receptor. Formation of disulfide bonds between I229C and A288C decrease I229C/A288C receptor responses to glycine, indicating that normal movement of TM1 and TM3 is required for gating. Reduction of the disulfide bond or mercury-linked dimer with DTT largely restores normal receptor function.

Disulfide bond formation between I229C and A288C is not spontaneous; instead, I229C/A288C receptors require either an oxidizing or a cross-linking agent to cross-link. In our previous cross-linking study of the S267C/A288C GlyR double mutant, S267C and A288C spontaneously formed disulfide bonds during channel gating without addition of a cross-linking or oxidizing reagent (Lobo *et al.* 2004b). The I229C/A288C receptors may require an oxidizing or cross-linking agent because these two residues face one another in a more hydrophobic environment, and both iodine and mercuric chloride enable cross-linking of cysteines in areas with a low dielectric constant. Alcohol and anesthetic-binding sites share common characteristics and are water-filled cavities with an amphipathic nature (Kruse *et al.* 2003; Bertaccini *et al.* 2007). Part of the drug-binding cavity has polar characteristics, with S267 in TM2, and possibly Y410 in TM4, contributing polar interactions to the binding cavity. Cysteines introduced at both of these sites were shown to be water-accessible and to react with sulfhydryl-specific compounds (Mascia *et al.* 2000; Lobo *et al.* 2004a, 2006). In addition to A288 and I229, W407 in TM4 was also shown to react with sulfhydryl-specific compounds (Lobo *et al.* 2006). These amino acids are non-polar and likely contribute hydrophobic interactions to stabilize binding of alcohol and anesthetic molecules. The non-polar environment surrounding I229 and A288 may also explain why the polar DTT molecule is not completely effective in accessing and reducing disulfide bonds between I229C and A288C.

Following cross-linking of I229C and A288C, the I229C/A288C receptors displayed tonic activity in a manner similar to previous manipulations, which introduced constraints and volume additions into this drug-binding cavity. For instance, spontaneous cross-linking between S267C and A288C in S267C/A288C GlyRs also resulted in tonically active channels (Lobo *et al.* 2004b). Mutation of amino acids in the drug-binding cavity to larger amino acids, such as S267I in GlyRs and S270W in $GABA_A$ α2 receptors, has been shown to cause constitutive receptor activity (Findlay *et al.* 2001; Beckstead *et al.* 2002). Reaction of long-chain sulfhydryl specific reagents with S267C in GlyRs resulted in tonic activity (Lobo *et al.* 2004a), and reaction of these molecules at the aligned position in the $5HT_3$ receptor also resulted in channels that were locked in the open state (Reeves *et al.* 2001). In all of these cases, stabilized receptor function resulted from alterations at positions hypothesized to be involved with drug binding. A recent study showed that occupation of even a single drug-binding cavity per receptor enhanced GlyR function (Roberts *et al.* 2006). These results suggest that subtle changes as a result of drug binding can preferentially stabilize different channel states. Here, we observed decreased I229C/A288C receptor function following cross-linking, suggesting that restricted movement of TM1 and TM3 locked channels in both open and desensitized states, thereby preventing channels from closing and re-sensitizing properly. Reduction with DTT largely restored the normal dynamic channel activity.

Previous mutational studies showed that increasing the volume of side chains at I229, S267, and A288 (or the corresponding residues in the $GABA_AR$ α1) decreased the 'cutoff' volume of small molecules that potentiated these receptors (Wick *et al.* 1998; Jenkins *et al.* 2001). Our molecular modeling of GlyRs and $GABA_ARs$ suggested that we interpret the results of these mutations in terms of a common binding site within the center of a four-helical bundle (Yamakura *et al.* 2001; Lobo *et al.* 2004a; Bertaccini *et al.* 2005a; Lobo and Harris 2005). As a result of these previous findings, our initial hypothesis was that I229 would face into the center of each subunit. As shown in Fig. 6b, this hypothesis was supported by the experimental cross-linking data.

The structure and function of TM1, in particular the extracellular half between G221 and P230, has been the subject of much interest. Its importance in function has been extensively studied because of the naturally occurring hyperekplexia mutation of G221 (Rajendra *et al.* 1997). The 'Pre-TM1' segment preceding G221 also has been studied extensively (Castaldo *et al.* 2004; Keramidas *et al.* 2006). We previously used the C-terminal segment of the AChBP (Brejc *et al.* 2001) to orient the ligand-binding domain of the GlyR and $GABA_AR$ with respect to the center of the TM1 alpha helix (Trudell and Bertaccini 2004). The relative orientation of the Pre-TM1 segment in the AChBP was recently confirmed in a high-resolution crystal structure of the nAChR (Dellisanti *et al.* 2007). This beta strand segment is barely long enough to reach between the ligand binding and the TM domains. Therefore, it is likely that there is some tension on the upper part of the TM1 alpha helix and this tension may distort the helical structure and result in the irregular labeling results previously reported with photolabeling (Blanton *et al.* 1994), cysteine mutagenesis (Akabas and Karlin 1995), and mass spectrometry (Leite *et al.* 2000).

In experiments using limited proteolysis of the GlyR, coupled with mass spectrometry, cleavage sites were noted in TM1 (Leite *et al.* 2000). The authors suggested these short fragments were more consistent with a beta sheet structure rather than an alpha helix (Leite *et al.* 2000; Leite and Cascio 2001). Use of the substituted cysteine accessibility method in the AChR resulted in an irregular pattern of reactivity, leading to the hypothesis that the most extracellular portion of TM1 along with TM2 contributed to the channel pore (Akabas and Karlin 1995). The irregular labeling pattern of several lipophilic photoactivable reagents was inconsistent with the pattern for either a classic alpha helix or a beta sheet and was compatible with a distorted or non-linear alpha helix or pleated beta sheet structure (Blanton and Cohen 1994; Blanton *et al.* 1998b; Barrantes 2003). Incorporation of a lipophilic photoactivatable probe was restricted to amino acids cytoplasmic of proline in the *Torpedo* AChR (Blanton *et al.* 1998a). Studies in the nAChR α2 subunit using nuclear magnetic resonance predicted that the TM1 alpha helix begins two residues before the proline and that the proline promotes non-helical structure in this region (Bondarenko *et al.* 2007).

For these reasons, it is possible that TM1 in the GlyR has some non-helical structure. In part, this distorted structure may be caused by a kink at the evolutionarily conserved proline located near the center of TM1. Our previous model of the TM domain utilized a four-helical bundle with an 18 degree left supertwist (Trudell and Bertaccini 2004). This supertwist caused the upper region of TM1 to tip into the ion channel pore and become part of the lining. Interestingly, the fulcrum point of this tipping is P230. Proline residues commonly serve as switch motifs within TM alpha helices of signaling proteins (reviewed in Sansom and Weinstein 2000). It has been proposed that P229 in TM1 of the homologous $5HT_{3A}$ receptor could undergo a *cis-trans* isomerization, thereby changing the orientation of the extracellular half of TM1 (Dang *et al.* 2000; Lester *et al.* 2004). This flexibility and 'kinking' could be partly responsible for the wringing behavior observed in analyses of the dynamics of these receptors (Bertaccini *et al.* 2005b; Paas *et al.* 2005).

Prolines have an inflexible ring structure and lack the capacity to hydrogen bond, which makes them uncommon in alpha helices. The structure surrounding P230 is therefore uncertain. Previously, mutations of this conserved proline in both $5HT_{3A}$ receptors and nAChRs resulted in channels with abnormal gating. The authors suggested that introduction of an additional hydrogen bond, by replacing the backbone proline, produced an inflexible TM1 secondary structure (England *et al.* 1999; Dang *et al.* 2000). Consistent with these studies, we found that mutation of this proline resulted in an abnormal P230C/A288C receptor with poor expression, extremely low currents, and high desensitization, suggesting that this position is also conserved for a critical purpose in GlyR function.

Both M227C and S231C single mutants reacted with iodine, resulting in decreased receptor function. We established that these two introduced cysteines did not cross-link with either A288C or the native C290, but we are not able to define plausible cysteine 'partners' for bond formation in these mutants. Cross-linking has previously identified inter-subunit contact points in the $GABA_A$ receptor between adjacent or non-adjacent subunits across the pore in TM2 (Horenstein *et al.* 2001; Bera *et al.* 2002; Rosen *et al.* 2007; Yang *et al.* 2007). Additionally, it has been shown that functional channels can be formed in which pore-forming residues in adjacent subunits are cross-linked, even though the three-dimensional structure of these channels must be highly strained. For instance, the C-alpha to C-alpha distance of $GABA_AR$ alpha1 H109C in the corresponding structure of nAChR (PDB ID 2BG9) is approximately 15 Å (Sarto-Jackson *et al.* 2007). The distance is far greater that the optimal distance for a di-cysteine cross-link of 6 Å. Nevertheless, the channels open with reduced ion current and respond to benzodiazepines (Sarto-Jackson *et al.* 2007). It is possible that M227C (or S231C) bind to another M227C (or S231C) to form disulfides with a neighboring subunit across the pore. A second possibility is that M227C (or S231C) cross-link with another membrane protein. Further studies are necessary to define the structure of TM1 in GlyRs.

Sequence homology is low between GlyRs/$GABA_A$Rs and nAChRs within TM3. Based on a consensus of ten bioinformatics techniques, Bertaccini and Trudell (2002) suggested a single gap after GlyR K281 in the alignment of residues between the extracellular end of TM2 and the intracellular end of TM3 in the nAChR. However, Sieghart and coworkers proposed that the $GABA_AR$ should have two gaps inserted before TM3 in the alignment with the nAChR (Ernst *et al.* 2005; Sarto-Jackson *et al.* 2007). Each gap would have the effect of moving GlyR A288 100 degrees clockwise toward the center of the subunit. The present results (Figs 6 and 7) clearly support the two-gap alignment proposed by Sieghart and coworkers. This alignment positions A288C toward the center of the four-helical bundle where it could cross-link to I229C and well as to S267C (Lobo *et al.* 2004b).

These data show the proximity of amino acids I229 and A288 in the GlyR because the I229C/A288C double mutant can form disulfide bonds during channel gating when exposed to an oxidizing or cross-linking agent. Disulfide bond formation between these two sites defines the positioning of TM1 and TM3. This provides strong evidence that I229 and A288 contribute to a binding cavity for alcohols and volatile anesthetics that is located at the core of the GlyR α1 subunit's alpha helical bundle.

Acknowledgements

This study was supported by NIH grants AA06399 (RAH), AA013378 (JRT), GM47818 (RAH), and AA007471-20 (IAL). The authors thank Chang Hoon Lee and Dr Wayne Hubbell for helpful discussions and assistance.

Abbreviations used

$5\text{-}HT_{3A}$
5-hydroxytryptamine type 3A

AChBP
acetylcholine-binding protein

AChR
acetylcholine receptor

DTT
dithiothreitol

$GABA_AR$
GABA type A receptor

GlyR
glycine receptor

MBS
modified Barth's solution

nAChR
nicotinic acetylcholine receptor

TM
transmembrane

WT
wild-type

References

Akabas MH, Karlin A. Identification of acetylcholine receptor channel-lining residues in the M1 Segment of the alpha-subunit. Biochemistry 1995;34:12496–12500. [PubMed: 7547996]

Barrantes FJ. Modulation of nicotinic acetylcholine receptor function through the outer and middle rings of transmembrane domains. Curr Opin Drug Discov Dev 2003;6:620–632.

Beckstead MJ, Phelan R, Trudell JR, Bianchini MJ, Mihic SJ. Anesthetic and ethanol effects on spontaneously opening glycine receptor channels. J Neurochem 2002;82:1343–1351. [PubMed: 12354281]

Bera AK, Chatav M, Akabas MH. GABAA receptor M2-M3 loop secondary structure and changes in accessibility during channel gating. J Biol Chem 2002;277:43002–43010. [PubMed: 12226083]

Bertaccini E, Trudell JR. Predicting the transmembrane secondary structure of ligand-gated ion channels. Protein Eng 2002;15:443–453. [PubMed: 12082162]

Bertaccini E, Shapiro J, Brutlag D, Trudell JR. Homology modeling of a human glycine alpha 1 receptor reveals a plausible anesthetic binding site. J Chem Inf Model 2005a;45:128–135. [PubMed: 15667138]

Bertaccini E, Trudell JR, Lindahl E. Normal mode analysis reveals the channel gating motion within a ligand gated ion channel model. Int Cong Ser 2005b;1283:160–163.

Bertaccini EJ, Trudell JR, Franks NP. The common chemical motifs within anesthetic binding sites. Anesth Analg 2007;104:318–324. [PubMed: 17242087]

Bertaccini EJ, Lindahl E, Trudell JR. Normal mode analysis of the Glycine alpha 1 receptor by three separate methods. J Chem Inf Model 2007;47:1572–1579. [PubMed: 17602605]

Betz H, Laube B. Glycine receptors: recent insights into their structural organization and functional diversity. J Neurochem 2006;97:1600–1610. [PubMed: 16805771]

Blanton MP, Cohen JB. Identifying the lipid-protein interface of the Torpedo nicotinic acetylcholine receptor: secondary structure implications. Biochemistry 1994;33:2859–2872. [PubMed: 8130199]

Blanton MP, Li YM, Stimson ER, Maggio JE, Cohen JB. Agonist-induced photoincorporation of a p-benzoylphenylalanine derivative of substance P into membrane-spanning region 2 of the Torpedo nicotinic acetylcholine receptor delta subunit. Mol Pharmacol 1994;46:1048–1055. [PubMed: 7528876]

Blanton MP, Dangott LJ, Raja SK, Lala AK, Cohen JB. Probing the structure of the nicotinic acetylcholine receptor ion channel with the uncharged photoactivable compound 2-[3H]diazofluorene. J Biol Chem 1998a;273:8659–8668. [PubMed: 9535841]

Blanton MP, McCardy EA, Huggins A, Parikh D. Probing the structure of the nicotinic acetylcholine receptor with the hydrophobic photoreactive probes [125I]TID-BE and [125I]TIDPC/16. Biochemistry 1998b;37:14545–14555. [PubMed: 9772183]

Bocquet N, Prado de Carvalho L, Cartaud J, Neyton J, Le Poupon C, Taly A, Grutter T, Changeux J-P, Corringer PJ. A prokaryotic proton-gated ion channel from the nicotinic acetylcholine receptor family. Nature 2007;445:116–119. [PubMed: 17167423]

Bondarenko V, Xu Y, Tang P. Structure of the first trans-membrane domain of the neuronal acetylcholine receptor β2 subunit. Biophys J 2007;92:1616–1622. [PubMed: 17142275]

Brejc K, van Dijk WJ, Klaassen RV, Schuurmans M, van Der OJ, Smit AB, Sixma TK. Crystal structure of an ACh-binding protein reveals the ligand-binding domain of nicotinic receptors. Nature 2001;411:269–276. [PubMed: 11357122]

Campagna-Slater V, Weaver DF. Molecular modelling of the GABAA ion channel protein. J Mol Graph Model 2007;25:721–730. [PubMed: 16877018]

Castaldo P, Stefanoni P, Miceli F, et al. A novel hyperekplexia-causing mutation in the pre-transmembrane segment 1 of the human glycine receptor alpha1 subunit reduces membrane expression and impairs gating by agonists. J Biol Chem 2004;279:25598–25604. [PubMed: 15066993]

Cheng MH, Cascio M, Coalson RD. Homology modeling and molecular dynamics simulations of the alpha1 glycine receptor reveals different states of the channel. Proteins 2007a;68:581–593. [PubMed: 17469203]

Cheng X, Ivanov I, Wang H, Sine SM, McCammon JA. Nanosecond-timescale conformational dynamics of the human α7 nicotinic acetylcholine receptor. Biophys J 2007b;93:2622–2634. [PubMed: 17573436]

Crawford DK, Trudell JR, Bertaccini EJ, Li K, Davies DL, Alkana RL. Evidence that ethanol acts on a target in Loop 2 of the extracellular domain of alpha1 glycine receptors. J Neurochem 2007;102:2097–2109. [PubMed: 17561937]

Dang H, England PM, Farivar SS, Dougherty DA, Lester HA. Probing the role of a conserved M1 proline residue in 5-hydroxytryptamine(3) receptor gating. Mol Pharmacol 2000;57:1114–1122. [PubMed: 10825381]

Dellisanti CD, Yao Y, Stroud JC, Wang Z-Z, Chen L. Crystal structure of the extracellular domain of nAChR [alpha]1 bound to [alpha]-bungarotoxin at 1.94 Å resolution. Nat Neurosci 2007;10:953–962. [PubMed: 17643119]

England PM, Zhang Y, Dougherty DA, Lester HA. Backbone mutations in transmembrane domains of a ligand-gated ion channel: implications for the mechanism of gating. Cell 1999;96:89–98. [PubMed: 9989500]

Ernst M, Bruckner S, Boresch S, Sieghart W. Comparative models of GABAA receptor extracellular and transmembrane domains: important insights in pharmacology and function. Mol Pharmacol 2005;68:1291–1300. [PubMed: 16103045]

Findlay GS, Ueno S, Harrison NL, Harris RA. Allosteric modulation in spontaneously active mutant gamma-aminobutyric acidA receptors. Neurosci Lett 2001;305:77–80. [PubMed: 11356312]

Hemmings HC Jr, Akabas MH, Goldstein PA, Trudell JR, Orser BA, Harrison NL. Emerging molecular mechanisms of general anesthetic action. Trends Pharmacol Sci 2005;26:503–510. [PubMed: 16126282]

Horenstein J, Wagner DA, Czajkowski C, Akabas MH. Protein mobility and GABA-induced conformational changes in GABA(A) receptor pore-lining M2 segment. Nat Neurosci 2001;4:477–485. [PubMed: 11319555]

Hughson AG, Lee GF, Hazelbauer GL. Analysis of protein structure in intact cells: crosslinking in vivo between introduced cysteines in the transmembrane domain of a bacterial chemoreceptor. Protein Sci 1997;6:315–322. [PubMed: 9041632]

Jenkins A, Greenblatt EP, Faulkner HJ, et al. Evidence for a common binding cavity for three general anesthetics within the GABAA receptor. J Neurosci 2001;21:RC136. [PubMed: 11245705]

Jung S, Harris RA. Sites in TM2 and 3 are critical for alcohol-induced conformational changes in GABA receptors. J Neurochem 2006;96:885–892. [PubMed: 16405501]

Jung S, Akabas MH, Harris RA. Functional and structural analysis of the GABAA receptor alpha 1 subunit during channel gating and alcohol modulation. J Biol Chem 2005;280:308–316. [PubMed: 15522868]

Keramidas A, Kash TL, Harrison NL. The pre-M1 segment of the alpha1 subunit is a transduction element in the activation of the GABAA receptor. J Physiol 2006;575:11–22. [PubMed: 16763005]

Kruse SW, Zhao R, Smith DP, Jones DN. Structure of a specific alcohol-binding site defined by the odorant binding protein LUSH from *Drosophila melanogaster*. Nat Struct Biol 2003;10:694–700. [PubMed: 12881720]

Lee GF, Dutton DP, Hazelbauer GL. Identification of functionally important helical faces in transmembrane segments by scanning mutagenesis. Proc Natl Acad Sci USA 1995a;92:5416–5420. [PubMed: 7777522]

Lee GF, Lebert MR, Lilly AA, Hazelbauer GL. Transmembrane signaling characterized in bacterial chemoreceptors by using sulfhydryl cross-linking in vivo. Proc Natl Acad Sci USA 1995b;92:3391–3395. [PubMed: 7724572]

Leite JF, Cascio M. Structure of ligand-gated ion channels: critical assessment of biochemical data supports novel topology. Mol Cell Neurosci 2001;17:777–792. [PubMed: 11358478]

Leite JF, Amoscato AA, Cascio M. Coupled proteolytic and mass spectrometry studies indicate a novel topology for the glycine receptor. J Biol Chem 2000;275:13683–13689. [PubMed: 10788487]

Lester HA, Dibas MI, Dahan DS, Leite JF, Dougherty DA. Cys-loop receptors: new twists and turns. Trends Neurosci 2004;27:329–336. [PubMed: 15165737]

Lobo IA, Harris RA. Sites of alcohol and volatile anesthetic action on glycine receptors. Int Rev Neurobiol 2005;65:53–87. [PubMed: 16140053]

Lobo IA, Mascia MP, Trudell JR, Harris RA. Channel gating of the glycine receptor changes accessibility to residues implicated in receptor potentiation by alcohols and anesthetics. J Biol Chem 2004a; 279:33919–33927. [PubMed: 15169788]

Lobo IA, Trudell JR, Harris RA. Cross-linking of glycine receptor transmembrane segments two and three alters coupling of ligand binding with channel opening. J Neurochem 2004b;90:962–969. [PubMed: 15287902]

Lobo IA, Trudell JR, Harris RA. Accessibility to residues in transmembrane segment four of the glycine receptor. Neuropharmacology 2006;50:174–181. [PubMed: 16225893]

Mascia MP, Mihic SJ, Valenzuela CF, Schofield PR, Harris RA. A single amino acid determines differences in ethanol actions on strychnine-sensitive glycine receptors. Mol Pharmacol 1996;50:402–406. [PubMed: 8700149]

Mascia MP, Trudell JR, Harris RA. Specific binding sites for alcohols and anesthetics on ligand-gated ion channels. Proc Natl Acad Sci USA 2000;97:9305–9310. [PubMed: 10908659]

Mihic SJ, Ye Q, Wick MJ, et al. Sites of alcohol and volatile anaesthetic action on GABA(A) and glycine receptors. Nature 1997;389:385–389. [PubMed: 9311780]

Miyazawa A, Fujiyoshi Y, Unwin N. Structure and gating mechanism of the acetylcholine receptor pore. Nature 2003;423:949–955. [PubMed: 12827192]

Ortells MO, Lunt GG. Evolutionary history of the ligand-gated ion-channel superfamily of receptors. Trends Neurosci 1995;18:121–127. [PubMed: 7754520]

Paas Y, Gibor G, Grailhe R, Savatier-Duclert N, Dufresne V, Sunesen M, de Carvalho LP, Changeux JP, Attali B. Pore conformations and gating mechanism of a Cys-loop receptor. Proc Natl Acad Sci USA 2005;102:15877–15882. [PubMed: 16247006]

Purohit P, Mitra A, Auerbach A. A stepwise mechanism for acetylcholine receptor channel gating. Nature 2007;446:930–933. [PubMed: 17443187]

Rajendra S, Lynch JW, Schofield PR. The glycine receptor. Pharmacol Ther 1997;73:121–146. [PubMed: 9131721]

Reeves DC, Goren EN, Akabas MH, Lummis SC. Structural and electrostatic properties of the 5-HT3 receptor pore revealed by substituted cysteine accessibility mutagenesis. J Biol Chem 2001;276:42035–42042. [PubMed: 11557761]

Roberts MT, Phelan R, Erlichman BS, Pillai RN, Ma L, Lopreato GF, Mihic SJ. Occupancy of a single anesthetic binding pocket is sufficient to enhance glycine receptor function. J Biol Chem 2006;281:3305–3311. [PubMed: 16361257]

Rosen A, Bali M, Horenstein J, Akabas MH. Channel opening by anesthetics and GABA induces similar changes in the GABAA receptor M2 segment. Biophys J 2007;92:3130–3139. [PubMed: 17293408]

Sansom MSP, Weinstein H. Hinges, swivels and switches: the role of prolines in signalling via transmembrane [alpha]-helices. Trends Pharmacol Sci 2000;21:445–451. [PubMed: 11121576]

Sarto-Jackson I, Furtmueller R, Ernst M, Huck S, Sieghart W. Spontaneous cross-link of mutated alpha1 subunits during GABA(A) receptor assembly. J Biol Chem 2007;282:4354–4363. [PubMed: 17148454]

Soskine M, Steiner-Mordoch S, Schuldiner S. Crosslinking of membrane-embedded cysteines reveals contact points in the EmrE oligomer. Proc Natl Acad Sci USA 2002;99:12043–12048. [PubMed: 12221291]

Taleb O, Betz H. Expression of the human glycine receptor alpha 1 subunit in *Xenopus* oocytes: apparent affinities of agonists increase at high receptor density. EMBO J 1994;13:1318–1324. [PubMed: 8137816]

Taly A, Delarue M, Grutter T, Nilges M, Le Novere N, Corringer PJ, Changeux JP. Normal mode analysis suggest a quaternary twist model for the nicotinic receptor gating mechanism. Biophys J 2005;88:3954–3965. [PubMed: 15805177]

Trudell JR, Bertaccini E. Comparative modeling of a GABAA a1 receptor using three crystal structures as templates. J Mol Graph Model 2004;23:39–49. [PubMed: 15331052]

Unwin N. Refined structure of the nicotinic acetylcholine receptor at 4A resolution. J Mol Biol 2005;346:967–989. [PubMed: 15701510]

Wick MJ, Mihic SJ, Ueno S, Mascia MP, Trudell JR, Brozowski SJ, Ye Q, Harrison NL, Harris RA. Mutations of GABA and glycine receptors change alcohol cutoff: evidence for an alcohol receptor? Proc Natl Acad Sci USA 1998;95:6504–6509. [PubMed: 9600996]

Winston SE, Mehan R, Falke JJ. Evidence that the adaptation region of the aspartate receptor is a dynamic four-helix bundle: cysteine and disulfide scanning studies. Biochemistry 2005;44:12655–12666. [PubMed: 16171380]

Yamakura T, Mihic SJ, Harris RA. Amino acid volume and hydropathy of a transmembrane site determine glycine and anesthetic sensitivity of glycine receptors. J Biol Chem 1999;274:23006–23012. [PubMed: 10438467]

Yamakura T, Bertaccini E, Trudell JR, Harris RA. Anesthetics and ion channels: molecular models and sites of anesthetic action. Ann Rev Pharmacol Toxicol 2001;41:23–51. [PubMed: 11264449]

Yang K, Farrens DL, Altenbach C, Farahbakhsh ZT, Hubbell WL, Khorana HG. Structure and function in rhodopsin. Cysteines 65 and 316 are in proximity in a rhodopsin mutant as indicated by disulfide formation and interactions between attached spin labels. Biochemistry 1996;35:14040–14046. [PubMed: 8916888]

Yang Z, Webb TI, Lynch JW. Closed-state crosslinking of adjacent beta 1 subunits in alpha 1beta 1 GABA-A receptors via 6′introduced cysteines. J Biol Chem 2007;282:16803–16810. [PubMed: 17405880]

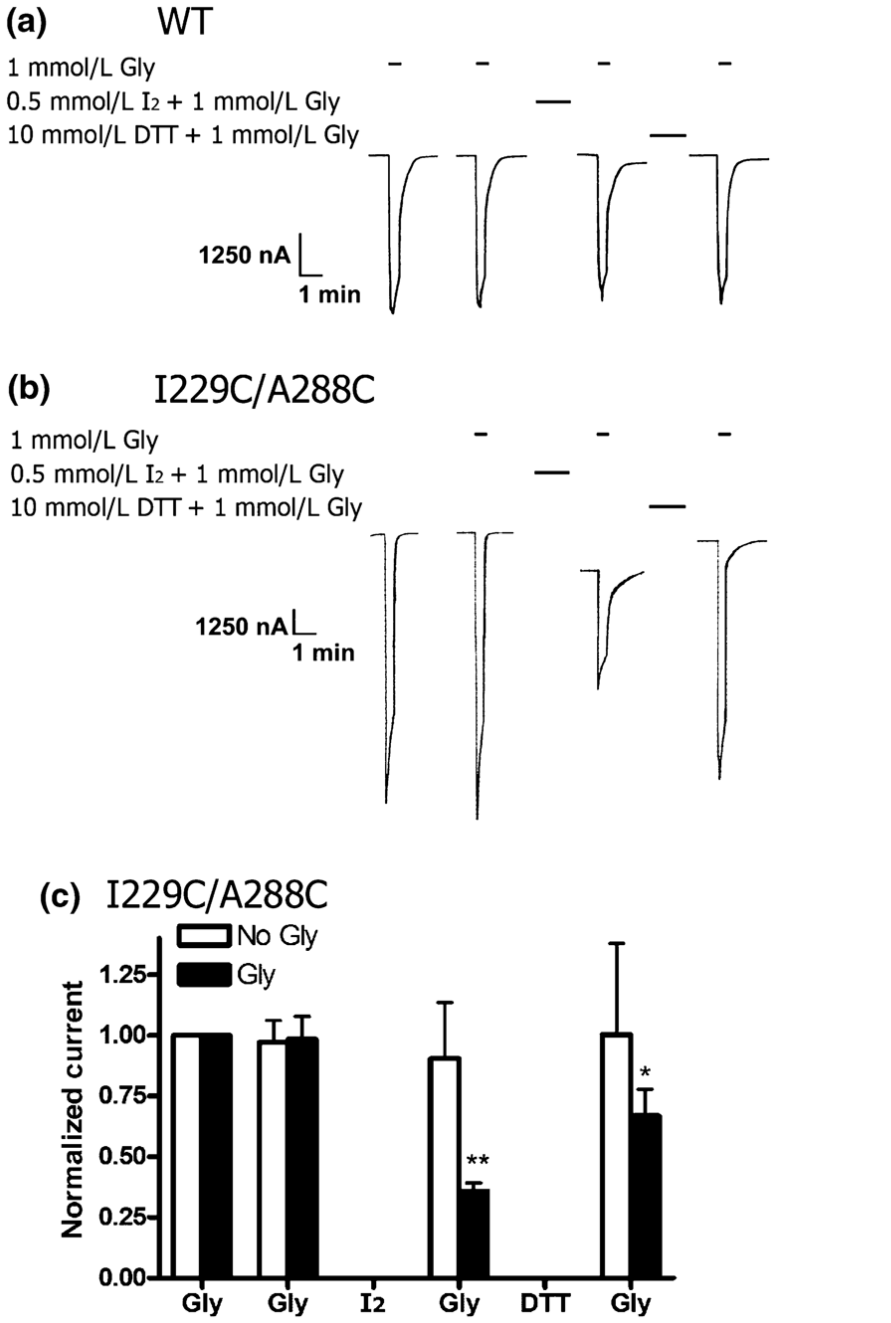

Fig. 1.

Effect of oxidation with iodine and reduction with DTT on WT and 1229C/A288C glycine receptors. (a) A WT tracing, which shows that the glycine response is unchanged by application of I_2 (0.5 mmol/L, 1 min) and DTT (10 mmol/L, 3 min) in the presence of glycine (1 mmol/L). Oocytes were unclamped during I_2 and DTT treatment, so this portion of the tracing is not shown. The intervals between each treatment is 15 min. (b) An I229C/A288C tracing, which shows that the glycine response decreases following application of I_2 (0.5 mmol/L, 1 min) in the presence of 1 mmol/L glycine and recovers after treatment with DTT (10 mmol/L, 3 min). (c) I229C/A288C cross-linking with I_2 in the absence or presence of glycine (1 mmol/L). Mean results showing that I_2 applied in the presence of glycine (Gly) results in a significant decrease

in the I229C/A288C receptor response because of disulfide bond formation ($n = 5$). Reduction with DTT nearly restores the glycine response to the initial amplitude. Disulfide bond formation did not occur when I_2 was applied in the absence of glycine (No Gly, $n = 7$). Glycine responses of each oocyte were normalized to the initial glycine response and averaged. Subsequent glycine responses were compared with the respective initial glycine response by one-way ANOVA and the Dunnett's post-test (*$p < 0.05$ and **$p < 0.01$).

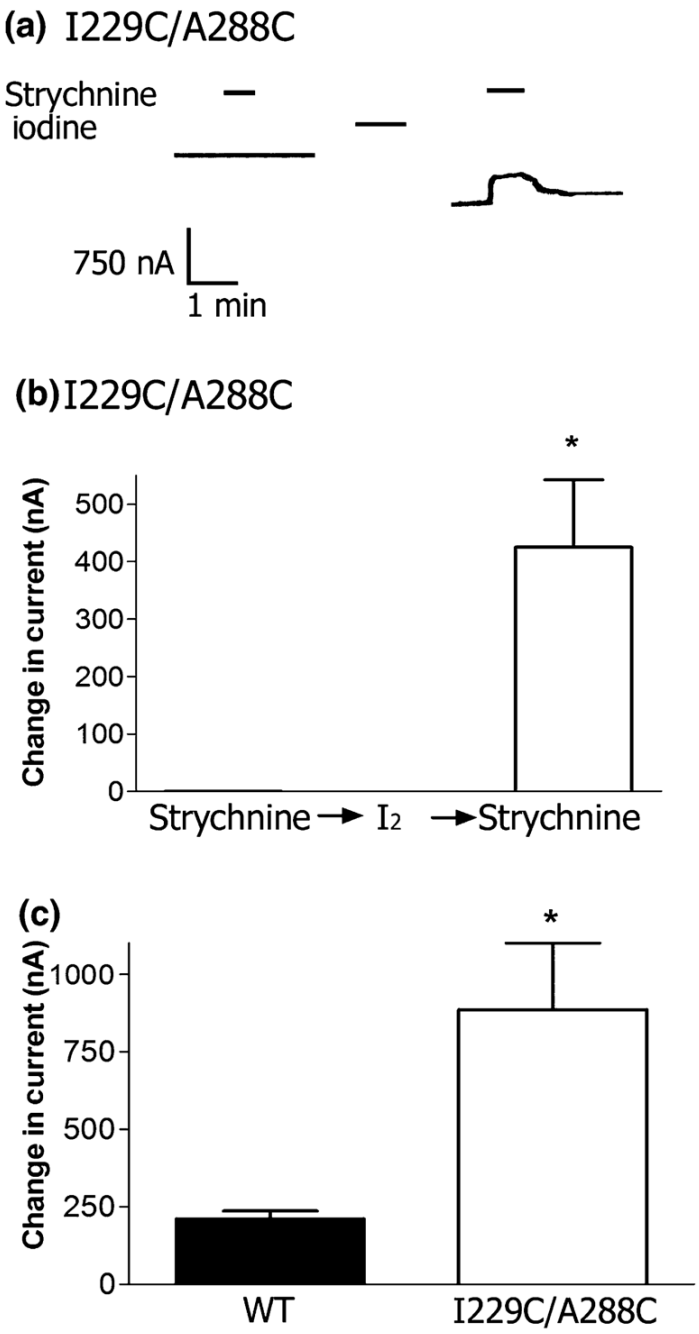

Fig. 2.

Cross-linking of I229C and A288C results in tonic activity and a baseline shift. (a) While WT receptors do not respond to applications of strychnine (10 μmol/L, 40 s) either before or after application of I_2 (0.5 mmol/L, 1 min), I229C/A288C receptors show tonic activity following cross-linking with iodine. Application of 10 μmol/L strychnine (40 s) has no effect on I229C/A288C receptors before cross-linking, and results in a decrease in tonic inward current following cross-linking, as shown in the tracing. (b) The mean effect of strychnine (10 μmol/L) on I229/A288C receptors before and after cross-linking with 0.5 mmol/L iodine ($n = 5$ oocytes per condition from two batches of oocytes). *$p < 0.05$ when compared with the effect before reduction by the Student's t-test. (c) The baseline current shifted in I229C/A288C

receptors after application of I_2 as an increase in inward current. The change in baseline of the WT was significantly smaller than for the I229C/A288C receptor. Mean values ± SEM are shown for $n = 5$ oocytes per condition from two batches of oocytes $*p < 0.05$ when compared with the WT using the Student's t-test.

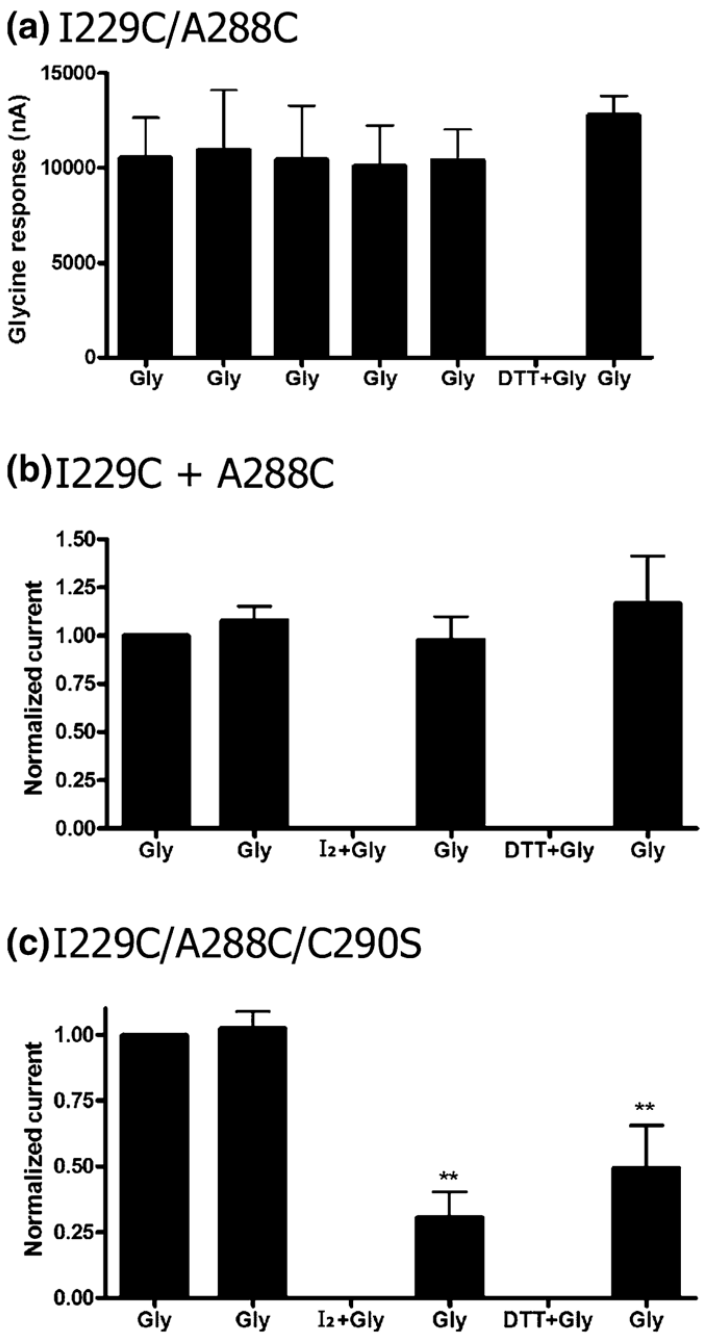

Fig. 3.

Auto-oxidation and intersubunit cross-linking do not occur between I229C and A288C. (a) Auto-oxidation does not occur in the I229C/A288C receptors with repeated applications of glycine (Gly; 1 mmol/L, 20 s) in the absence of an oxidizing or cross-linking agent. Glycine was applied five times at 15 min intervals, and there was no change in current over time. Exposure to DTT (10 mmol/L) in 1 mmol/L glycine did not increase the current of a subsequent glycine application. $n = 4$. (b) Application of iodine (0.5 mmol/L) in the presence of glycine does not change the maximal glycine response (10 mmol/L) in oocytes co-injected with I229C and A288C single mutant receptors (1:1 ratio), indicating that intersubunit cross-linking does not occur ($n = 4$). (c) I229C/A288C/C290S shows a reduced glycine response following

application of iodine (0.5 mmol/L) in the presence of glycine (n = 6). Glycine responses in (b and c) were normalized for each oocyte to the initial response and averaged. Subsequent glycine responses were compared with the respective initial glycine response by one-way ANOVA and the Dunnett's post-test.

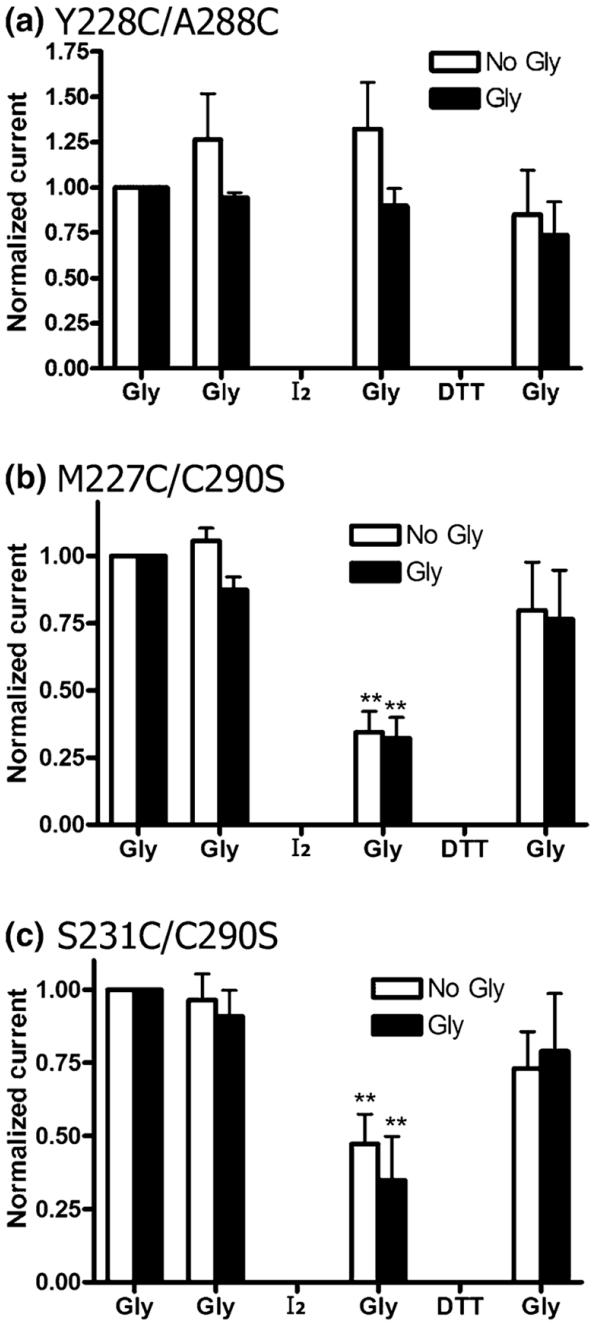

Fig. 4.

Cross-linking does not occur in the Y228C/A288C double mutant, and both M227C/C290S and S231C/C290S show reduced glycine responses following iodine treatment. Iodine and DTT were applied in the presence (Gly) or absence (No Gly) of glycine. (a) In Y228C/A288C receptors, there is no significant change in the glycine response following treatment with iodine (0.5 mmol/L) or DTT (10 mmol/L) in the presence or absence of 10 mmol/L glycine. (b) M227C/C290S receptors showed a decrease in current after treatment with of I_2 (0.5 mmol/L, 1 min). Currents were largely restored following treatment with DTT (10 mmol/L, 3 min) in the absence or presence of glycine (1 mmol/L). (c) Likewise, S231C/C290S receptors also showed a decrease in current after treatment with of I_2 (0.5 mmol/L, 1 min), and had restored

currents following treatment with DTT (10 mmol/L, 3 min) in the absence or presence of glycine (10 mmol/L). Glycine responses of each oocyte were normalized to the initial glycine response and averaged for $n = 4–8$ oocytes from two to four batches of oocytes. Subsequent glycine responses were compared with the respective initial glycine response by one-way ANOVA and the Dunnett's post-test (**$p < 0.01$).

```
2BG9_A|AChRa1  198 YLDITYHFIMQRIPLYFVVNVIIPCLLFSFLTVLVFYLPTDSG--- 240
P23415|GLRA1   209 CIEARFHLERQMG----YYLIQMYIPSLLIVILSWISFWINMDAAP 250

2BG9_A|AChRa1  241 EKMTLSISVLLSLTVFLLVIVELIPSTSSAVPLIGKYMLFTMIFVISSIIVTVVVIN 297
P23415|GLRA1   251 ARVGLGITTVLTMTTQSSGSRASLPKVSYVK--AIDIWMAVCLLFVFSALLEYAAVN 305

TM3-TM4 intracellular loop omitted

2BG9_A|AChRa1  400 KYVAMVIDHILLCVFMLICIIGTVSVFAG---RLIELSQEG 437
P23415|GLRA1   386 KIDKISRIGFPMAFLIFNMFYWIIYKIVR---REDVHNQ 421
```

Fig. 5.

Alignment of the TM domains of GlyR and nAChR. We aligned the primary sequences of torpedo nAChR alpha (PDB ID 2BG9) with human GlyR alpha1 (accession number P23415). Residues numbers of the mature proteins are given at the beginning and end of each line. Dashes represent gaps where there is no matching residue. The cytoplasmic loop that connects TM3 and TM4 was omitted for clarity. Three dashes indicate the end of TM4 and the beginning of a short C-terminus. We found that the combination of a model with two gaps after GlyR G221 and two gaps after K281 (Fig. 5) produced the shortest C-alpha to C-alpha distance for I229C/A288C (12.4 Å, Fig. 6b).

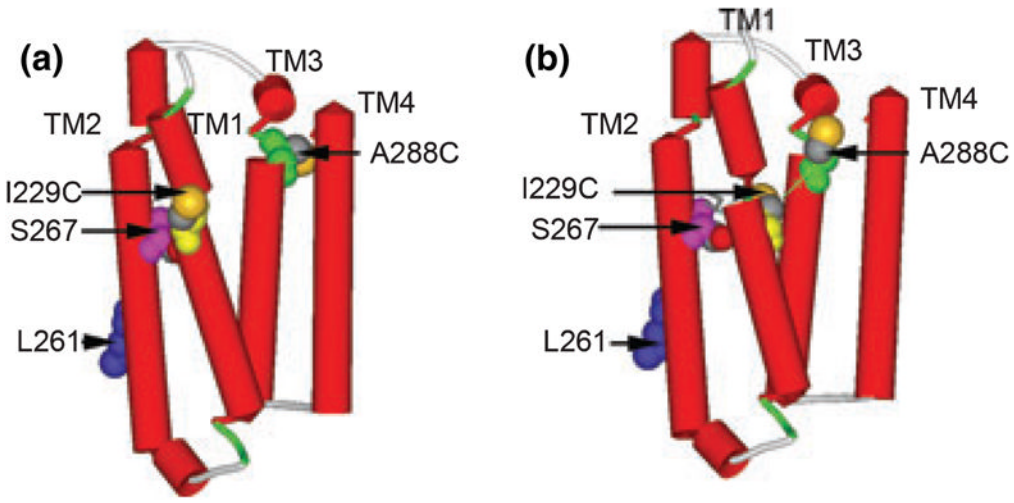

Fig. 6.

Molecular models of the TM domain of GlyRs. (a) The TM domain with the sequence of GlyR threaded directly onto the structure of nAChR (PDB ID 2BG9) with a previously suggested alignment (Bertaccini and Trudell 2002). The following residues were rendered with space filling surfaces: I229C is yellow, Leu261 (9′as a marker of a pore-lining residue) is blue, S267 is pink, A288C is green, and sulfur atoms are highlighted in orange. (b) The TM domain with the same residues after insertion of two gaps after Gly221 and one additional gap after Lys281. That is, GlyR Ile229 that was aligned with nAChR Ile220 in (a) is now aligned with Cys222 and GlyR A288 that was aligned with nAChR Leu279 in (a) is now aligned with Phe280. The thin green line shows the C-alpha to C-alpha dimension of 12.4 Å between I229C and A288C.

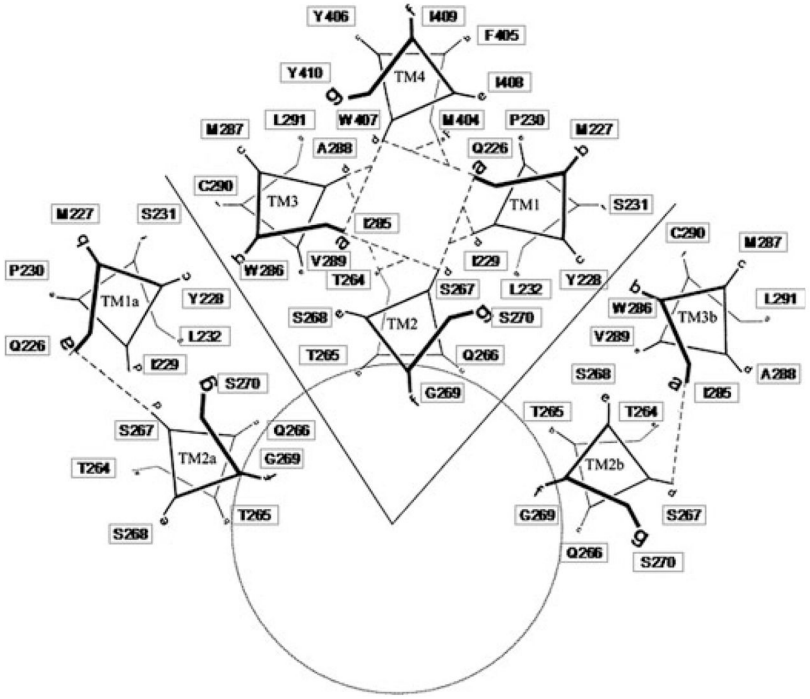

Fig. 7.

Helical wheel diagram of the TM domain of GlyRs. A helical wheel of a four-helical bundle was prepared and then duplicate images were added with a 72 degree rotation about the ion pore axis to form a homopentamer. In the present diagram, four heptads of one GlyR subunit were retained as well as the two counterclockwise heptads (TM1a and TM2a) and two clockwise heptads (TM2b and TM3b). The position of each residue in the eight heptads was linked to an Excel spreadsheet. This arrangement allowed ‘what if’ experiments by cutting and pasting residues in the spreadsheet and then updating the links. The present arrangement reflects the alignment in Fig. 5 and the two-gap model shown in Fig. 6. The residues most important for effects of alcohols and anesthetics were assigned a ‘D’ position in each heptad (I229, S267, A288, and W407).

Table 1

Glycine EC_{50} values, Hill coefficients, and maximal (Max) glycine responses for the WT receptor, and single, double and triple mutant GlyRs

GlyRα1	EC50 (μmol/L glycine)	Hill coefficient	Max current (μA)	*n*
WT	180 ± 56	2.6 ± 0.2	10.0 ± 3.1	10
I229C	110 ± 7.0	3.5 ± 0.5	3.5 ± 1.6	7
A288C	1800 ± 190**	2.1 ± 0.3	10.0 ± 2.2	5
I229C/A288C	180 ± 37	2.6 ± 0.3	9.5 ± 2.1	5
I229C/A228C/C290S	81 ± 4.5	2.2 ± 0.4	12.1 ± 2.6	5
C290S	120 ± 20	2.0 ± 0.2	11.2 ± 3.4	7
Y228C/A288C	1900 ± 210**	2.1 ± 0.1	4.1 ± 2.3	5
P230C/A288C	ND	ND	ND	0
M227C	250 ± 50	2.3 ± 0.4	6.2 ± 1.8	5
M227C/A288C	2200 ± 530**	3.2 ± 1.0	7.1 ± 3.8	5
M227C/C290S	200 ± 45	3.3 ± 0.8	10.5 ± 3.6	8
S231C	980 ± 240*	1.6 ± 0.2	11.0 ± 3.6	6
S231C/A288C	3700 ± 650**	2.4 ± 0.5	1.5 ± 0.6	5
S231C/C290S	730 ± 83	1.8 ± 0.2	6.9 ± 2.7	6

* $p < 0.05$ and

** $p < 0.01$ significantly different from WT receptor by one-way ANOVA with the Dunnett's post-test. The average glycine EC_{50} and Hill coefficients were calculated from fits of concentration–response curves from single oocytes, and the maximal currents for each receptor are expressed as a mean ± SEM. ND, not determined; GlyR, glycine receptor; WT, wild-type.

Table 2

Effects of iodine oxidation and DTT reduction on normalized WT, I229C, A288C, I229C/A288C, I229C/A288C/C290S, and I229C + A288C GlyRs currents

GlyRα1	Gly	Gly (post-oxidation)	Gly (post-reduction)	*n*
Cross-linking (I_2) and reduction in the absence of glycine				
WT	0.95 ± 0.05	0.83 ± 0.15	1.14 ± 0.28	8
I229C	0.87 ± 0.04	1.01 ± 0.08	1.15 ± 0.16	6
A288C	1.20 ± 0.07	1.18 ± 0.10	0.98 ± 0.13	7
I229C/A288C	0.97 ± 0.09	0.91 ± 0.23	1.00 ± 0.38	7
Cross-linking (I_2) and reduction in maximal glycine				
WT	0.97 ± 0.08	0.93 ± 0.10	0.99 ± 0.14	6
I229C	0.96 ± 0.09	1.34 ± 0.25	0.90 ± 0.21	5
A288C	0.96 ± 0.09	0.85 ± 0.28	1.02 ± 0.38	5
I229C/A288C	0.98 ± 0.09	0.36 ± 0.03**	0.67 ± 0.11*	5
I229C/A228C/C290S	1.02 ± 0.07	0.31 ± 0.10**	0.49 ± 0.16**	6
I229C + A288C (1:1)	1.08 ± 0.07	0.98 ± 0.12	1.17 ± 0.25	6

* $p < 0.05$ and

** $p < 0.01$ significantly different from initial glycine response for each receptor by one-way ANOVA and the Dunnett's post-test. Two applications of maximal glycine were followed by oxidation with iodine (0.5 mmol/L, 1 min), maximal glycine, reduction with DTT (10 mmol/L, 3 min), and a final application of maximal glycine. Washout times were 15 min intervals between applications. Application of iodine and DTT were carried out in either the presence or absence of glycine. Cross-linking with iodine in the presence of glycine resulted in decreased receptor responses in only the I229C/A288C and I229C/A288C/C290S receptors. The glycine responses for each receptor type were normalized to the respective initial glycine response (1.00, not shown), and the data were averaged. Data are expressed as the mean ± SEM. DTT, dithiothreitol; GlyR, glycine receptor; WT, wild-type.

Table 3

Effects of mercuric chloride cross-linking and DTT reduction in the presence of glycine on normalized WT, I229C, A288C, and I229C/A288C GlyRs currents

GlyR*α*1	Gly	Gly (post-$HgCl_2$)	Gly (post-reduction)	*n*
Cross-linking ($HgCl_2$) and reduction in maximal glycine				
WT	0.94 ± 0.05	0.95 ± 0.10	0.97 ± 0.16	5
I229C	0.95 ± 0.05	0.98 ± 0.12	1.02 ± 0.15	5
A288C	0.94 ± 0.09	1.08 ± 0.27	1.19 ± 0.45	5
I229C/A288C	0.84 ± 0.07	0.29 ± 0.04**	0.84 ± 0.11	5

** $p < 0.01$ significantly different from initial glycine response (normalized to 1.00 and not shown) for each receptor by one-way ANOVA and the Dunnett's post-test. Two applications of maximal glycine were followed by cross-linking with mercuric chloride (10 μmol/L, 1 min), maximal glycine, reduction with DTT (10 mmol/L, 3 min), and a final application of maximal glycine. Washout times were 15 min intervals between applications. Mercuric chloride and DTT were applied in the presence of maximal glycine. Cross-linking with iodine in the presence of glycine resulted in decreased receptor responses in only the I229C/A288C receptors, and currents were restored following application of DTT. The glycine responses were normalized to the initial glycine response (1.00, not shown), and the data was averaged. Data are expressed as the mean ± SEM. DTT, dithiothreitol; GlyR, glycine receptor; WT, wild-type.

Table 4

Effects of iodine and DTT applied in either the absence or presence of glycine on normalized GlyR currents of TM1 and TM3 single and double mutant GlyRs

GlyRα1	Gly	Gly (post-oxidation)	Gly (post-reduction)	*n*
Cross-linking (I_2) and reduction in the absence of glycine				
C290S	0.91 ± 0.03	0.89 ± 0.07	0.90 ± 0.15	6
Y228C/A288C	1.27 ± 0.25	1.32 ± 0.26	0.85 ± 0.24	5
M227C	0.98 ± 0.05	0.37 ± 0.12*	0.71 ± 0.30	7
M227C/A288C	0.98 ± 0.07	0.18 ± 0.06**	0.33 ± 0.08**	5
M227C/C290S	1.06 ± 0.05	0.34 ± 0.08**	0.80 ± 0.18	8
S231C	0.90 ± 0.04	0.26 ± 0.07**	0.46 ± 0.07**	5
S231C/A288C	1.00 ± 0.18	0.44 ± 0.08*	0.56 ± 0.14	6
vS231C/C290S	0.96 ± 0.09	0.47 ± 0.10**	0.73 ± 0.13	7
Cross-linking (I_2) and reduction in maximal glycine				
C290S	0.96 ± 0.08	0.79 ± 0.07	0.84 ± 0.08	7
Y228C/A288C	0.94 ± 0.03	0.90 ± 0.10	0.74 ± 0.18	5
M227C	0.94 ± 0.04	0.15 ± 0.04**	0.67 ± 0.05**	6
M227C/A288C	1.07 ± 0.06	0.30 ± 0.06**	0.47 ± 0.05**	6
M227C/C290S	0.87 ± 0.05	0.32 ± 0.08**	0.76 ± 0.18	7
S231C	0.87 ± 0.04	0.42 ± 0.10**	0.87 ± 0.17	5
S231C/A288C	1.06 ± 0.10	0.53 ± 0.09**	0.74 ± 0.12	5
S231C/C290S	0.91 ± 0.09	0.35 ± 0.15**	0.79 ± 0.20	5

* $p < 0.05$ and

** $p < 0.01$ significantly different from initial glycine response (normalized to 1.00 and not shown) for each receptor by one-way ANOVA and the Dunnett's post-test. Two applications of maximal glycine were followed by oxidation with iodine (0.5 mmol/L, 1 min), maximal glycine, reduction with DTT (10 mmol/L, 3 min), and a final application of maximal glycine. Washout times were 15 min intervals between applications. Iodine and DTT were applied in either the presence or absence of glycine. Iodine had no effect on the Y228C/A288C and C290S mutants, but decreased receptor responses in all M227C- and S231C-containing receptors. Currents were in some cases restored following application of DTT. The glycine responses were normalized to the initial glycine response (1.00, not shown), and the data was averaged. Data are expressed as the mean ± SEM. DTT, dithiothreitol; GlyR, glycine receptor; TM, transmembrane WT, wild-type.